

Laboratory of Computational Physics

BY LUCA CASSIA

Dipartimento di Fisica, Università di Milano-Bicocca
I-20126 Milano, Italy

Email: l.cassia@campus.unimib.it

Table of contents

1 Hard-Core Molecular Dynamics in $2d$	1
1.1 Thermalization	2
1.2 Momentum Distribution	5
1.3 Phase Transition	6
1.4 Collision Times	7

1 Hard-Core Molecular Dynamics in $2d$

In this section we simulate the dynamics of a system of N identical spherical particles in two dimensions, subject to the hard-core central potential:

$$V(r) = \begin{cases} 0 & r > R \\ \infty & r \leq R \end{cases} \quad (1)$$

with $\sigma = 2R$ being the diameter of the particles. For convenience we decide to work with adimensional quantities and rescale all lengths by the size L of the box. In these units the volume of the box itself is rescaled to 1. For the same reason we take the mass of the particles to be the reference unit of mass. Periodic boundary conditions in both directions are implemented in order to reduce boundary effects due to the finite size of the system. This turns our box in a toroidal surface.

1.1 Thermalization

First we initialize the system positioning the particles (disks) on the sites of a regular square lattice as in (Fig.1). This type of circle packing has a *packing density* η (i.e., the proportion of the surface covered by the circles) of:

$$\eta = \frac{N \pi \sigma^2}{4L^2} \quad (2)$$

which takes its maximum value for $\sigma = L/\sqrt{N}$:

$$\eta_{\max} = \frac{\pi}{4} \approx 0.78539816339... \quad (3)$$

The highest-density lattice arrangement of circles in the plane is actually the hexagonal packing arrangement, with a maximal packing density of $\eta_h = \frac{\pi}{2\sqrt{3}} \approx 0.9069$. In fact we see that, a system with large η , spontaneously tends to arrange itself in such a way (Fig.1).

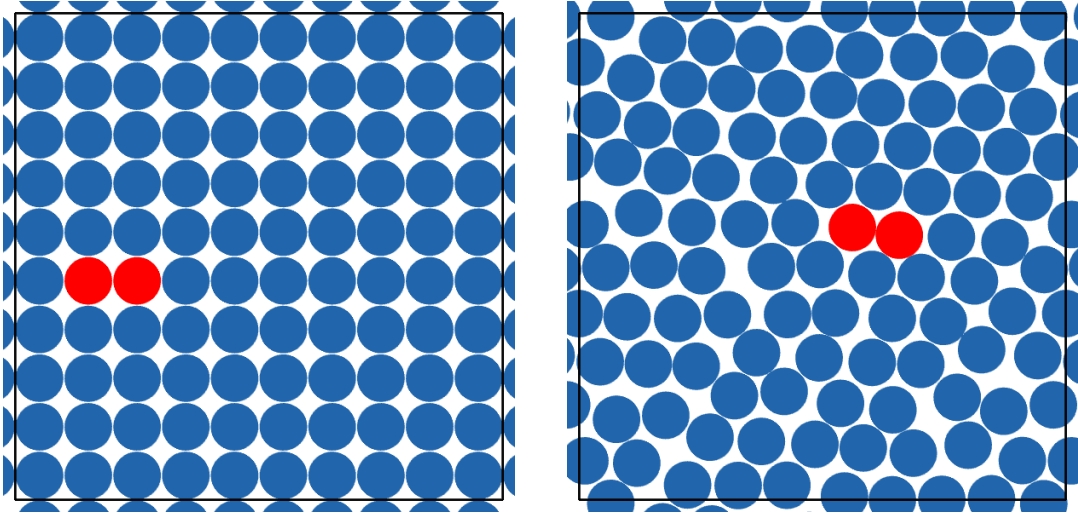


Figure 1. On the left we illustrate the initial spatial configuration of a system of 100 particles at temperature $T = 1$ and $\eta = 0.75$. On the right we show the same system after $2 \cdot 10^5$ collisions. The red disks indicate two particles colliding.

The momenta of the particles are initialized with uniform distribution inside the range $[-1, 1]$ with total momentum equal to zero (center of mass reference frame). After the initialization the momenta are rescaled in order to obtain the desired temperature. Kinetic energy and temperature are related by:

$$K = \frac{d}{2} N k_b T, \quad K = \frac{1}{2} m \sum_{i=1}^N |\vec{v}_i|^2 \quad (4)$$

$$\Rightarrow T = \frac{1}{d N} \sum_{i=1}^N |\vec{v}_i|^2 \quad (5)$$

where we set $k_b = 1 = m$.

We now study the mixing properties of this type of system. We evolve a system of $N = 100$ particles from its initial configuration, for 10^4 collisions and measure the pressure (Fig.2) and the mean free path (Fig.3) every 10 collisions. This procedure is also repeated for $N = 400$.

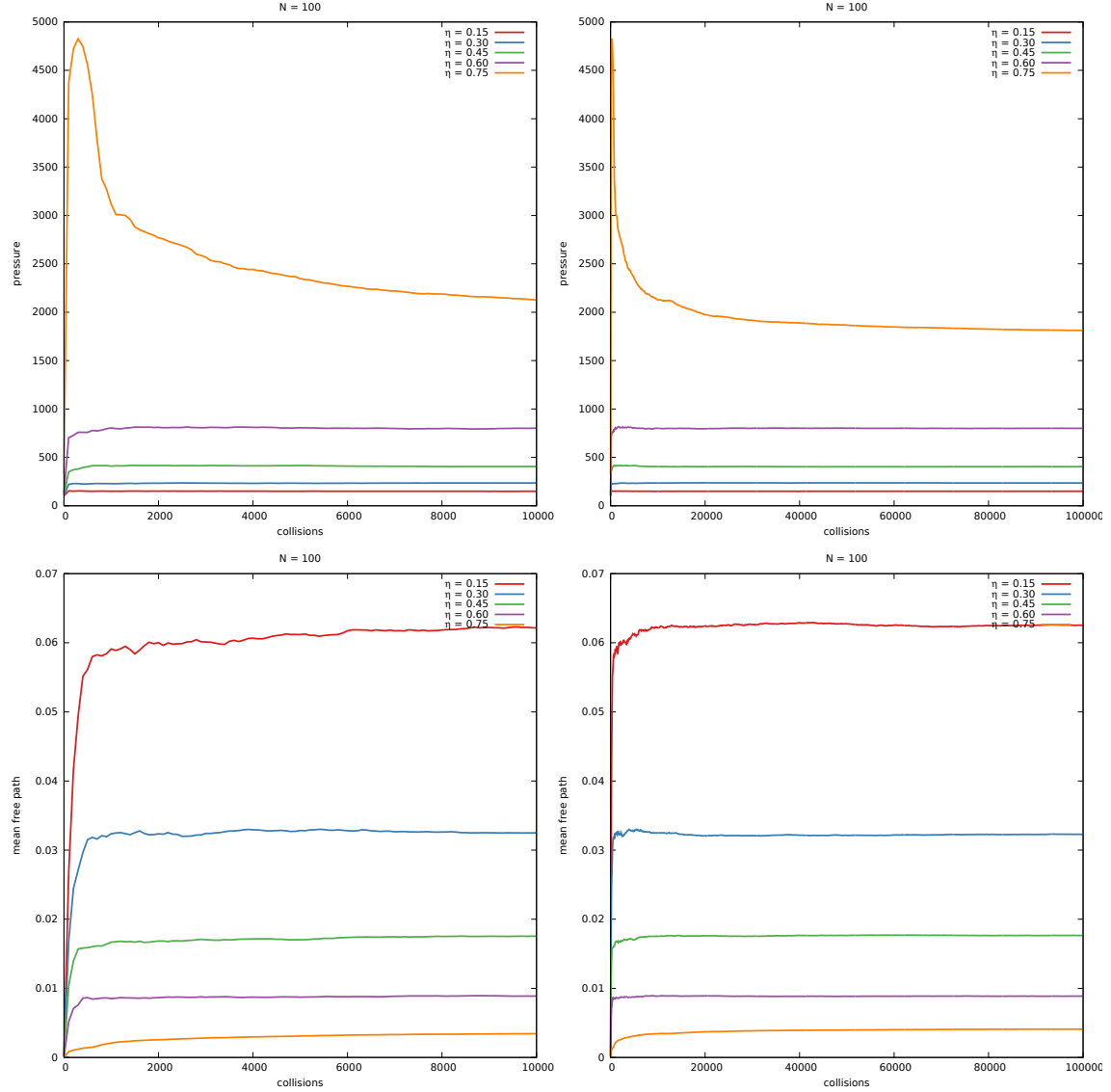


Figure 2. Plot of the thermalization process of an hard-core interacting gas of $N = 100$ particles. The top two figures illustrate the pressure as a function of the number of collisions, while the bottom two show the mean free path of the particles. Different colors represent the different values of $\eta = 0.15, 0.30, 0.45, 0.60, 0.75$ used for the simulations. On the right is the same process, after a larger number of collisions. The mixing rate of the system (as a function of the number of collisions) grows with η and the number of particles.

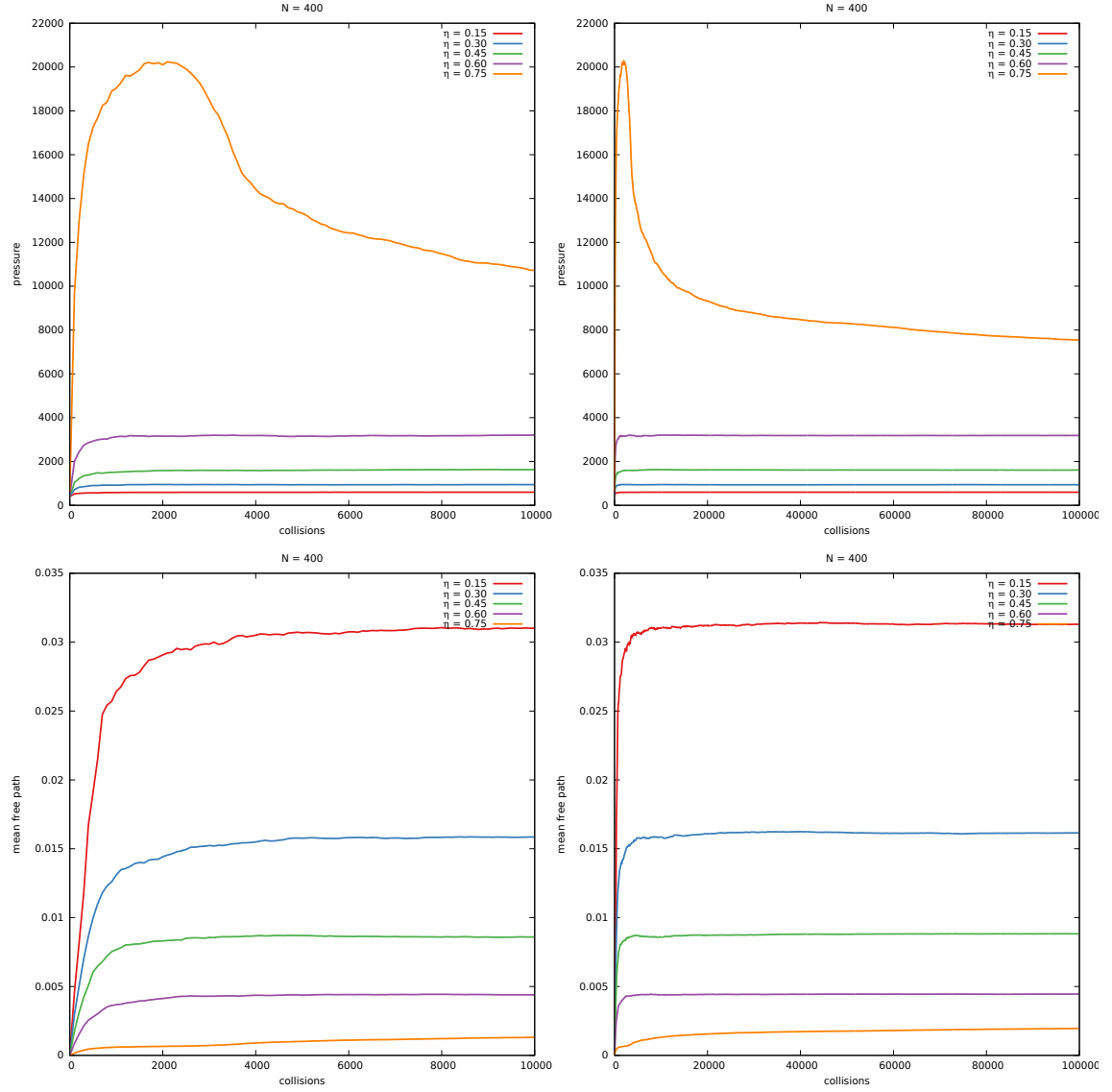


Figure 3. Plot of the thermalization process of an hard-core interacting gas of $N = 400$ particles. The mixing of this larger system is much slower.

A many-body system reaches thermalization only when every particle has interacted with every other particle at least once. Since hard-core particles interact only when they collide with each

other, the mixing of this type of systems depends only on the number of collisions and not directly on the elapsed time.

We see that larger systems (system with a large number of particles) need more collisions to mix completely, especially at high densities η , while smaller systems mix faster. At high densities we also note a peak in the pressure curve near the start of the simulation. This is due to the fact that we used an initial arrangement not ideal for the close packing of particles. The particles are initially very close to each other and interact frequently, but after a few collisions they rearrange in such a way as to maximize the distance between them, therefore reducing the pressure (Fig.1).

If we work with $N = 100$ particles, we can consider the system thermalized after $5 \cdot 10^5$ collisions.

1.2 Momentum Distribution

After thermalization is reached, the system acquires time translation invariance and the distribution of the momenta of the particles converge to the **Maxwell-Boltzmann distribution**:

$$f(v) = \sqrt{\left(\frac{m}{2\pi k_b T}\right)^3} 4\pi v^2 \exp\left[\frac{-m v^2}{2k_b T}\right] \quad (6)$$

and for the single components:

$$f(v_i) = \sqrt{\frac{m}{2\pi k_b T}} \exp\left[\frac{-m v_i^2}{2k_b T}\right] \quad (7)$$

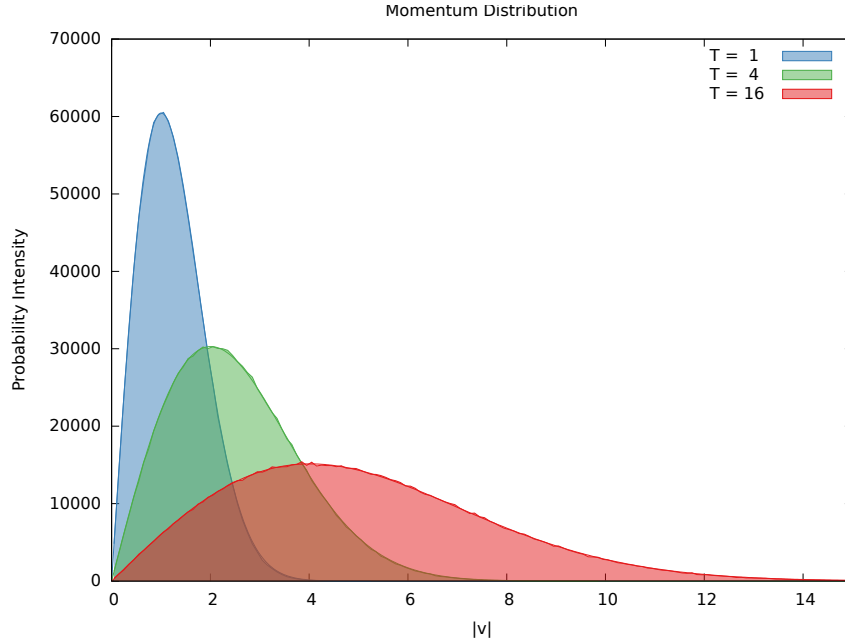


Figure 4. Histogram of the module of the momenta for $N = 100$ particles. The measurements are taken after 10^5 collisions from the start of the simulation, and after that every 500 collisions for a total of 10^4 datasets each containing the momenta of N particles. The system is initialized at temperatures $T = 1, 4, 16$.

We repeat the simulation for three different values of the temperature ($T = 1, 4, 16$) which we set by hand at the beginning. The temperature can then be read from a fit of the histograms of (Fig.4) and compared with the one obtained from (5):

T	T_{fit}
1	1.011343 ± 0.005696
4	4.028977 ± 0.007747
16	16.134445 ± 0.023048

We also plot the distribution for the single components v_x and v_y :

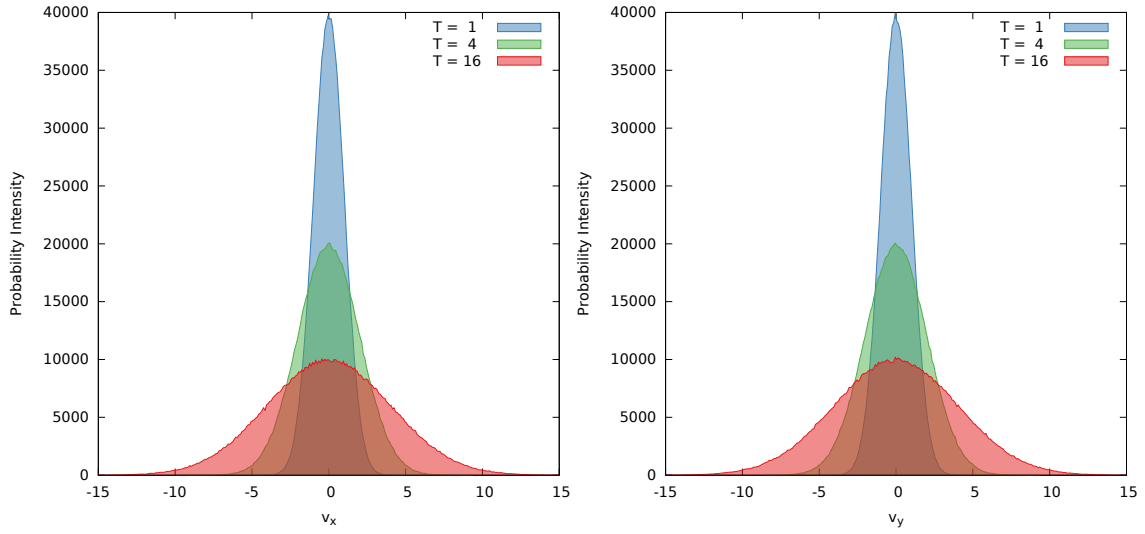


Figure 5. Histograms of the x (left) and y (right) components of the momenta for $N = 100$ particles.

1.3 Phase Transition

In this section we study the η dependence of some interesting quantities describing the system. First we look at the pressure P as the packing density is increased. For a system such as those in consideration, we define the pressure P using the formula:

$$\frac{PV}{Nk_bT} = 1 + \frac{1}{2Kt} \sum_{c=1}^{N_c} m \sigma |\Delta \vec{v}_{ij}(t_c)| \quad (8)$$

with $m\Delta\vec{v}_{ij}(t_c)$ being the exchanged momentum in the collision taking place at time t_c , N_c the total number of collisions and t the runtime of the simulation.

Remark: as a measure against autocorrelation effects we decide to sample data each from an independent run and then take the average over all runs (at the same η).

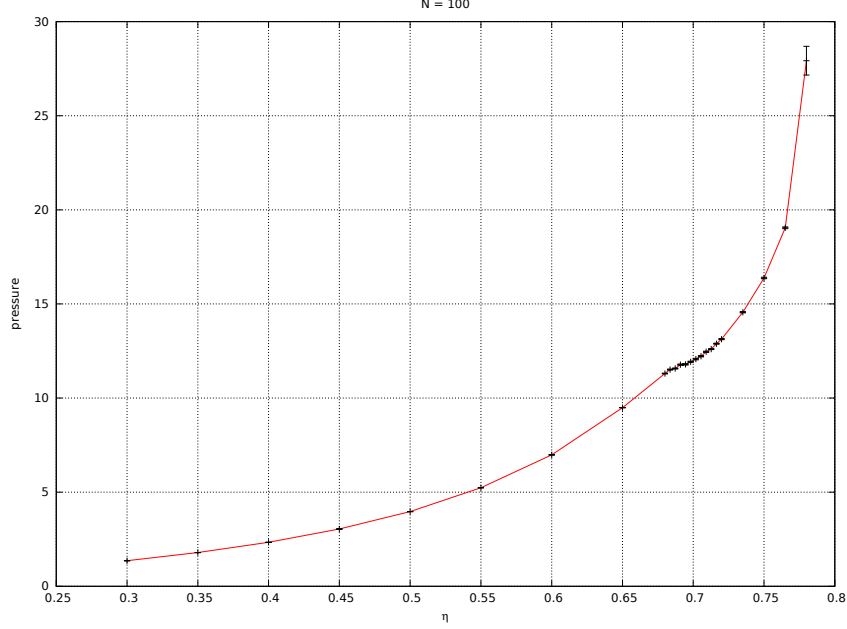


Figure 6. Plot of $\frac{PV}{NT} - 1$ as a function of η for a system of 100 particles. Every measurement is taken from the average of 50 independent runs each collected after an initial thermalization time of $5 \cdot 10^5$ collisions. The errorbars represent the standard errors of the averages.

Near $\eta = 0.7$ we observe a first order phase transition characterized by a discontinuity in the pressure with respect to the thermodynamic variable η . The system is found in a liquid phase for values of the density $\eta < 0.7$ and in a solid phase for $\eta > 0.7$. This kind of phase transition displays a plateau region where the transition takes place. In fact there is no well defined critical point since multiple phases can coexist near the transition.

We also note that, since the hard-core potential has no attractive effect on the particles, there cannot be a phase transition with respect to the temperature. The order-disorder transition we observe is purely of geometrical nature.

Another thermodynamic quantity that shows discontinuity at the phase transition is the mean free path, i.e., the average distance traveled by a particle between successive impacts:

$$l_c = \sum_{c=1}^{N_c} \frac{|\Delta\vec{r}_i(t_c, t_{c-1})|}{N_c} \quad (9)$$

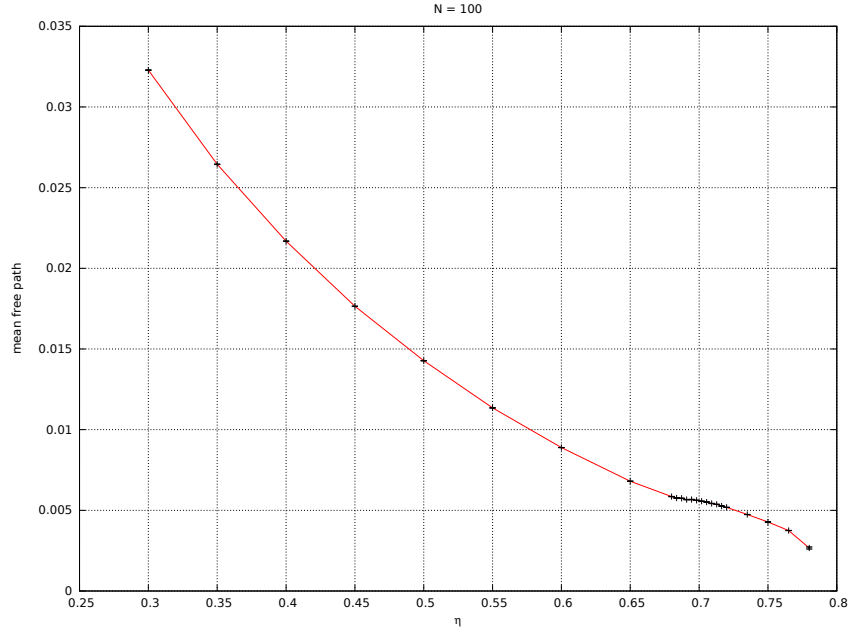


Figure 7. Plot of the mean free path against η for $N = 100$.

1.4 Collision Times

Another yet interesting quantity to look at is the collision time t_c , i.e., the time between two consecutive collisions. In (Fig.8) we present the distribution of t_c for increasing values of η :

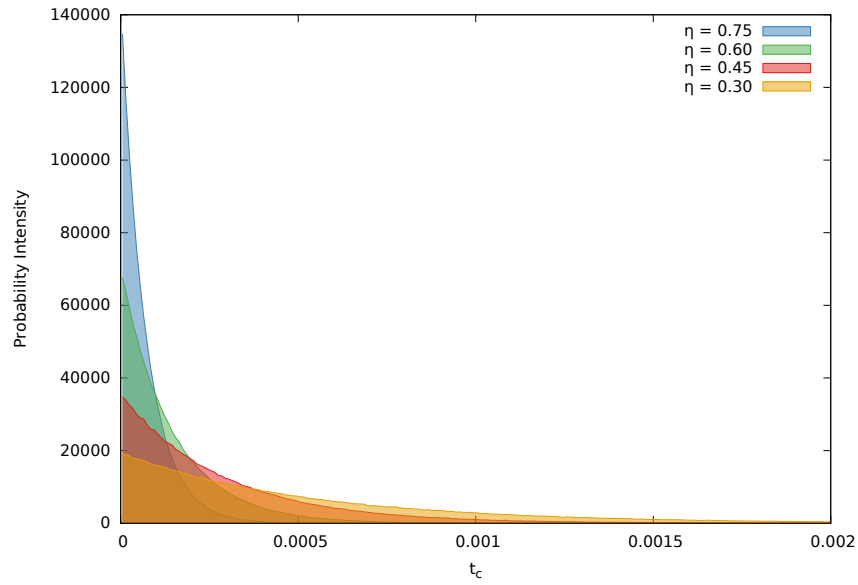


Figure 8. Distribution of the collision time t_c for $N = 100$ and $\eta = 0.30, 0.45, 0.60, 0.75$. The histograms are obtained from a sample of 10^6 measurements and after a thermalization time of $5 \cdot 10^5$ collisions.

As the density of particles increases, the collisions become more frequent because of the decrease in free space available for the particles to freely travel. This implies that the distribution of the collision times must become narrower for larger values of η (Fig.8).

Similarly to the case of the pressure and the mean free path, t_c also has a discontinuity at the phase transition, as we can see from (Fig.9):

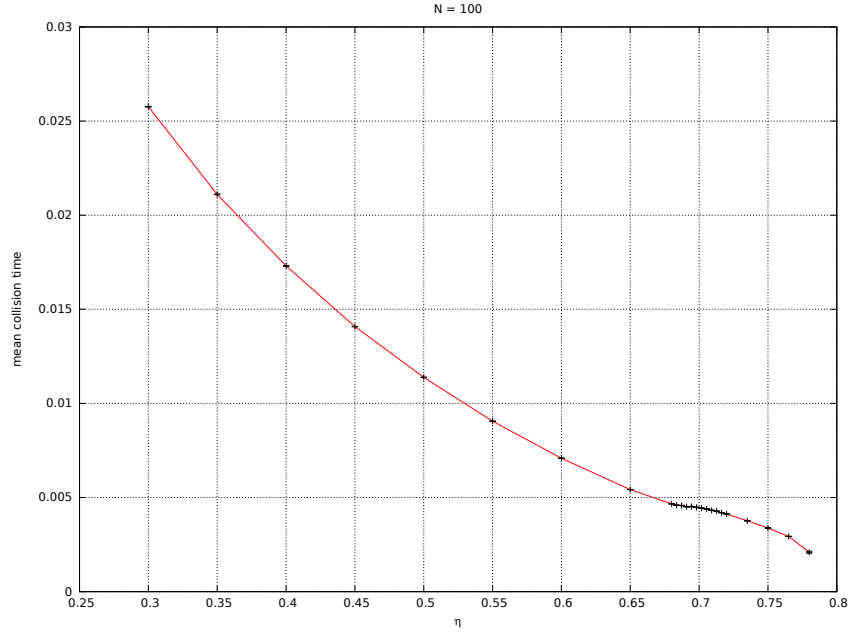


Figure 9. Plot of the mean collision time $\langle t_c \rangle$ against η for $N = 100$.